Channeling Effect and Tissue Morphology in a Perfusion Bioreactor Imaged by X-Ray Microtomography

Claire Beauchesne, Morgan Chabanon, Benjamin Smaniotto, Benoît Ladoux, Benoit Goyeau, Bertrand David

Channeling effect and tissue morphology in a perfusion bioreactor imaged by X-Ray microtomography

Channeling effect and tissue morphology under perfusion

Claire Beauchesne[1,2], Morgan Chabanon[3], Benjamin Smaniotto[4], Benoît Ladoux[5], Benoît Goyeau*[1], and Bertrand David[2]

[1]Lab. EM2C, UPR CNRS 288, CentraleSupélec, Univ. Paris-Saclay 3 Rue Joliot Curie, 91192 Gif-sur-Yvette Cedex France

[2]Lab. MSSMat, UMR CNRS 8579, CentraleSupélec, Univ. Paris-Saclay 3 Rue Joliot Curie, 91192 Gif-sur-Yvette Cedex France

[3]Single Molecule Biophotonics Lab. ICFO-The Institute of Photonic Sciences, av. Carl Friedrich Gauss, 3, 08860 Castelldefels, Barcelona, Spain

[4]ENS Paris Saclay, LMT, CNRS, UMR 8535, Cachan, France

[5]Institut Jacques Monod (IJM), UMR CNRS 7592, Univ. Paris Diderot, Paris, France

*Benoît Goyeau and Bertrand David should be considered joint senior authors.

Correspondance to: Pr. B. Goyeau, 3 rue Joliot-Curie 91190 Gif-sur-Yvette, +33 1 75 31 60 58, benoit.goyeau@centralesupelec.fr

Abstract

BACKGROUND:

Perfusion bioreactors for tissue engineering hold great promises. Indeed, the perfusion of culture medium enhances species transport and mechanically stimulates the cells, thereby increasing cell proliferation and tissue formation. Nonetheless, their development is still hampered by a lack of understanding of the relationship between mechanical cues and tissue growth.

METHODS:

Combining tissue engineering, three-dimensional visualization and numerical simulations, we analyze the morphological evolution of neo-tissue in a model bioreactor with respect to the local flow pattern. NIH-3T3 cells were grown under perfusion for one, two and three weeks on a stack of 2 mm polyacetal beads. The model bioreactor was then imaged by X-ray micro-tomography and local tissue morphology was analyzed. To relate experimental observations and mechanical stimulii, a computational fluid dynamics model of flow around spheres in a canal was developed and solved using the finite element method.

RESULTS:

We observe a preferential tissue formation at the bioreactor periphery, and relate it to a channeling effect leading to regions of higher flow intensity. Additionally, we find that, circular crater-like tissue patterns form in narrow channel regions at early culture times. Using computational fluid dynamic simulations, we show that the location and morphology of these patterns match those of shear stress maxima. Finally, the morphology of the tissue is qualitatively described as the tissue grows and reorganizes itself.

CONCLUSION:

Altogether, our study points out the key role of local flow conditions on the tissue morphology developed on a stack of beads in perfusion bioreactors and provides new insights for effective design of hydrodynamic bioreactors for tissue engineering using bead packings.

Key words: X-ray microtomography, perfusion bioreactor, tissue engineering, channeling effect, tissue morphology

1 Introduction

In the context of tissue engineering, several types of bioreactors have been designed in an attempt to enhance in vitro cell proliferation and differentiation in a dynamic and controlled environment: spinner flasks [1], rotating wall bioreactors [2], and perfusion systems [3, 4]. Yet an associated challenge is to provide homogeneous nutrients and oxygen supply within the whole volume of such scaffold. Perfusion bioreactors have been shown to give good results in this regard [5, 6], leading to relatively even cell seeding and growth on the porous scaffold [7, 8]. Perfusion bioreactors present a similar basic design consisting of a closed tubing circuit with a culture medium reservoir, a pump, and a growth chamber. They mainly differ in the design of the cell seeded-scaffold residing inside the growth chamber (fiber meshes, beads or cubes stacks, ...) and the scaffold materials (coral, titanium, alginate, starch-based material, calcium-phosphate ceramics, ...) [3, 9, 10].
Given the complex culture environment in perfusion bioreactors, where the fluid flow stimulates cell proliferation and tissue growth alters in turn the fluid flow, recent investigations have turned to modeling approaches to optimize their tissue production [11].

In hydrodynamic bioreactors, fluid flow alters cell differentiation and proliferation [5, 12] by providing a mechanical stimulation of the cells [3, 13] and enhancing species transport such as nutrients supply and waste removal [14, 15]. Externally applied forces, such as shear stresses, traction stresses or fluid drag [16], are translated into intracellular biochemical signaling, which results in a modification of the cellular response [17]. This process, termed mechanosensitivity, is at the origin of many important biological functions, including bone remodeling [18]. Mechanosensitive mechanisms have been identified such as the activation of stretch-activated ion channels [19, 20], integrin-initiated cytoskeleton deformations [21–23], and the stimulation of the primary cilia [24].
More generally, tissue pattern is driven by the complex combination of external signallings [25, 26]: the substrate material and local geometry (either the scaffold or the extracellular matrix), the culture medium (nutrients, growth factors, mitogens, etc...), and external forces (such as those applied by other cells or fluid shear stress). Besides fluid flow enhanced prolifer-

ation, the way connective cells colonize the scaffold is of paramount importance. Despite recent progress in the description of connective tissue growth or repair in static conditions [27–31], the mechanisms underlying its formation in dynamic conditions are still poorly understood. In particular, the morphology of a tissue growing under perfusion of culture medium as well as the distribution of cells within this tissue are key information for the development of bioreactors for tissue engineering.

Several studies adopted a modeling approach to understand the interplay between tissue growth and fluid flow. Numerical simulations of fluid flow through empty porous scaffolds have been performed in order to determine the shear stress field and predict the preferential locations of cell proliferation at the initiation of cell culture [4, 32, 33]. More complex models have been proposed to simulate the evolution of the fluid flow as tissue grows by addition of cell layers of varying thicknesses [34] or by using a moving boundary approach where the interfacial velocity is a function of the local fluid shear stress [35]. Recently, the experimental evidence that the geometry strongly influences the tissue morphology and growth kinetics in static conditions [29, 36] motivated the development of new models. Indeed, tissue growth kinetics under perfusion is determined as a function of both the curvature of the tissue growth front and the fluid shear stress [11, 37], although these predictions are still to be validated against experimental data at the pore scale. Overall, given the complexity of the biophysical phenomena at stakes in perfusion bioreactors, modeling and numerical simulations in simplified controlled settings, appear as valuable investigative tools.

In this study, we propose to take advantage of a model-system inspired from a perfusion bioreactor for bone tissue engineering [3] in order to describe the morphological evolution of neo-tissue with respect to local flow patterns. Our model system makes use of two main simplifications: (i) murine fibroblasts are chosen for their rapid proliferation rate, mechanosensitivity, and ability to produce connective tissue, and (ii) the scaffold is composed of immobile, impermeable and non-absorbable polyacetal beads in order to use a simple geometry and image the bioreactor by X-Ray micro-tomography. We combine three-dimensional visualization by X-Ray micro-tomography and computational fluid dynamic to answer the following questions: How does the

fluid flow pattern determine the spatial distribution of tissue in the bioreactor? What is the morphology of the tissue as it grows?

2 Materials and Methods

2.1 Cells

Fibroblasts NIH-3T3 (ATCC) were cultured in DMEM Glutamax (Life Technologies) supplemented with 10% Fetal Bovine Serum (Pan-Biotech) and 1% Penicillin Streptomycin (Pan-Biotech), at pH 7.4 under standard cell culture conditions (37 °C, 5% CO_2, 100% humidity). Following previous tissue engineering studies using murine fibroblasts [38–40], these cells have been chosen for our model system because they belong to the family of connective tissue cells (like chondrocytes, osteoblasts, ...) [41]. Additionally, they respond to mechanical stimuli [42], which is relevant to our perfusion bioreactor model and have a rapid proliferation rate.

2.2 Perfusion bioreactor

The perfusion bioreactor (Fig. 1) consists of a closed tubing circuit with a media reservoir, a peristaltic pump, and a perfusion chamber [3, 43]. The cylindrical growth chamber (13.8 mm diameter, 5 cm high, made of polycarbonate) is randomly filled by mono disperse polyacetal beads (2 mm diameter). Let us note that bead-based scaffolds have been identified as good candidates for tissue engineering and therefore have been investigated multiple times [4, 32, 39, 40, 44–47]. The beads are immobilized by two polycarbonate grids (0.5 cm high), inserted in the growth chamber at the bioreactor inlet and outlet. Polyacetal is semi-transparent to X-rays allowing the reconstruction of three-dimensional images of the tissue on the beads. In addition, the scaffold is immobile and non-absorbable: this allows to study tissue growth for a given bead stack arrangement. Finally, note that since the beads volume fraction remains constant, the local organization and the global height of bead stacks are slightly sample dependent. The chamber is closed by two caps made of polytetrafluoroethylene and a tubing made of silicon (Pharm-Med) connects the bioreactor to the culture medium reservoir. The culture medium pH is kept constant by the constant supply of air enriched with carbon dioxide at 5%.

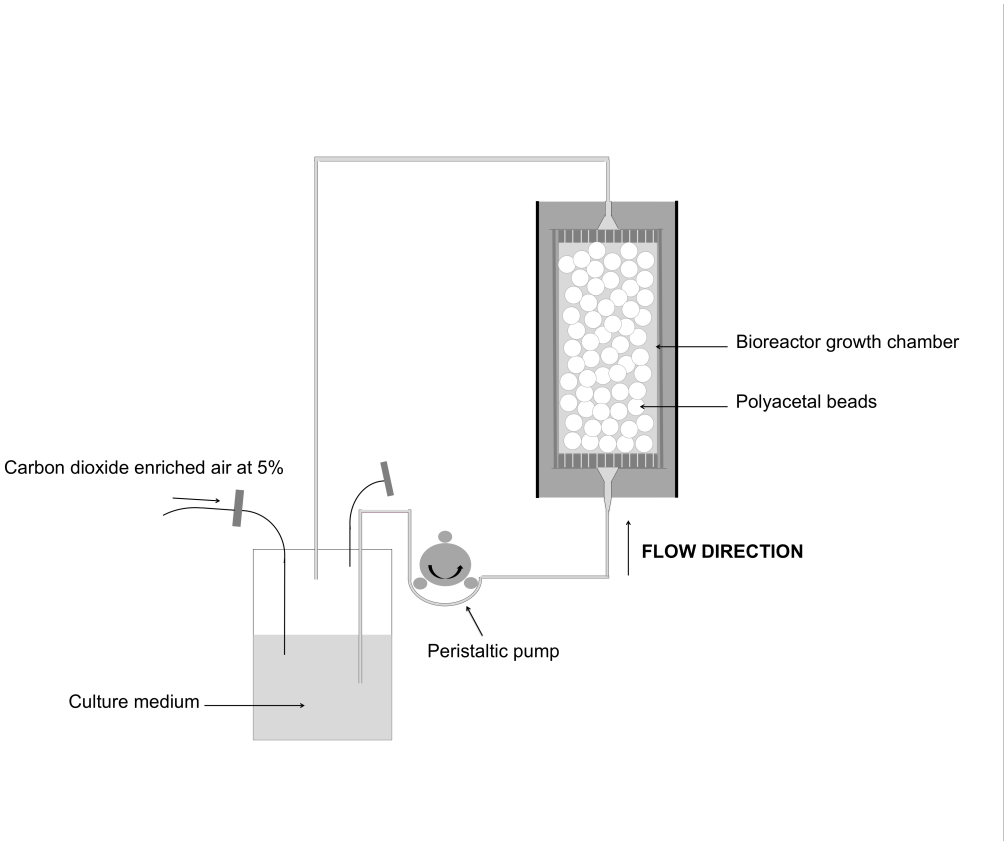

Figure 1: Schematic representation of the experimental set-up.

2.3 Dynamic cell culture in perfusion bioreactor

The following procedure has been followed in order to seed the cells on the beads before their introduction into the bioreactor [40, 48]. First, a suspension of pre-confluent NIH-3T3 cells (10^6 cells/ml) in culture medium was gently poured onto the polyacetal beads previously coated with fibronectin (10 μg/ml, 1 hour at 37°C), then left overnight in a CO_2 incubator to let the cells adhere to the beads. The seeded scaffold was then gently poured into the perfusion bioreactor and immobilized by two grids to avoid any bead movements during culture medium changes. The constructs were perfused at a constant flow rate of 20 ml/min or 30 ml/min for one, two or three weeks (two constructs per experimental condition). The culture medium was changed for the first time after one week then twice a week. At the indicated time points, the constructs, still immobilized by the two grids, were washed with PBS prior being fixed with 4% paraformaldehyde (Sigma-Aldrich) in PBS (Pan-Biotech), then washed again with PBS and H_2O prior being stained with 1% osmium tetroxide OsO_4 (Sigma-Aldrich) in H_2O. The solution is beforehand gently injected multiple times at the top and bottom of each sample through the peripheral envelop of tissue in order to ensure that the core of the samples are fully immersed

in the solution. The samples were then dehydrated through a series of ethanol baths of growing concentrations (50, 70, 90, 95, and 100%) before being dried using hexamethyldisilazane (Sigma-Aldrich). Osmium is a heavy metal that stains cell membranes thereby making cells visible by X-ray microtomography.

2.4 Visualization of the cellular phase

The stained cellular phase was imaged by an X-ray tomography system (North Star Imaging, NSI, X50-CT) equipped with a molybdenum target and a CMOS image sensor Dexela 2923. Two series of scans were performed with the following characteristics:

- Physical voxel length of 17 μm with a height of field view of about 2.8-2.9 cm and centered at mid-height of the bioreactor growth chamber. The voltage was 50 kV and the current 400 μA. 900 projections were obtained from each sample over 360 degrees.
- Physical voxel length of 10.2 μm with a height of field view of about 1.1 cm from the top or the bottom of the bioreactor growth chamber. The voltage was 50 kV and the current 230 μA. 1000 projections were obtained from each sample over 360 degrees.

2.5 Image analysis

The reconstruction was performed with efX-software (NSI) and image processing with ImageJ (version 1.51w) [49].

The mean intensity, that we define as the mean grey value, is measured on the raw data (16 bits) after subtracting the mean intensity of the background noise, measured outside the bioreactor.

The creation of a Region of Interest (ROI) delimiting the cellular regions in the parietal region and in the core of the bioreactor followed four steps:
Step 1: The mean intensity of the background noise, measured outside the bioreactor wall, was subtracted.
Step 2: The tube was removed by application of an inverted circular mask on all the slices. The

mask was created beforehand by drawing two ovals matching the inner perimeter of the tube on the first and last slide of the stack, and adding them to a ROI. The ROI was completed between the first and last slides by interpolation. The associated mask for the tube was then generated and applied to the stack of the samples obtained in step 1.

Step 3: A binary image of the cellular region was obtained in three steps. The thinnest tissue regions were selected by subtracting the background with rolling ball radius set to 1 then 2 pixels on duplicated stacks. Both stacks were added and thresholded to create a binary mask consisting of the regions where the tissue is the thinnest (Step 3a). The largest tissue regions were isolated by thresholding and converted to a mask (Step 3b). Both masks were added in order to obtain the cellular region as binary image (Step 3c).

Step 4: The annular and core regions were delimited by a radius R. A circle of radius R was drawn on the first and last slides with the same center as the centroid of the growth chamber wall and added to a ROI. The ROI was completed between the first and last slides by interpolation. The circular mask of radius R was then generated. For selecting the cellular region close to the bioreactor wall (or in the core), the mask (respectively the inverted mask) was applied to the binarised image defining the cellular region. The cellular region was finally selected with subpixel accuracy and added to a new ROI.

3 Results and discussion

Fibroblasts NIH-3T3 cells were cultured for one, two or three weeks in the bioreactor for two different perfusion flow rates of culture medium (20 or 30 ml/min). The samples were scanned by X-ray micro-tomography and the tridimensional arrangements of the beads and the tissue were obtained after image reconstruction. Preliminary experiments showed that tissue proliferation on glass and polyacetal bead stacks in static conditions (without flow) was negligible compared to dynamic conditions [39, 40], producing too little tissue volume to be resolved by X-ray microtomography. Additionally, mass transport estimates in similar culture conditions and close flow rate indicate that oxygen and nutrient supply is in excess during most of the three weeks of culture [39].

3.1 Channeling effect locally enhances the perfusion flow rate at the bead stack periphery

After two or three weeks of culture, we observe a preferential proliferation at the periphery of the bead stack where the cells form an external tissue envelope (Fig. 2a,b).

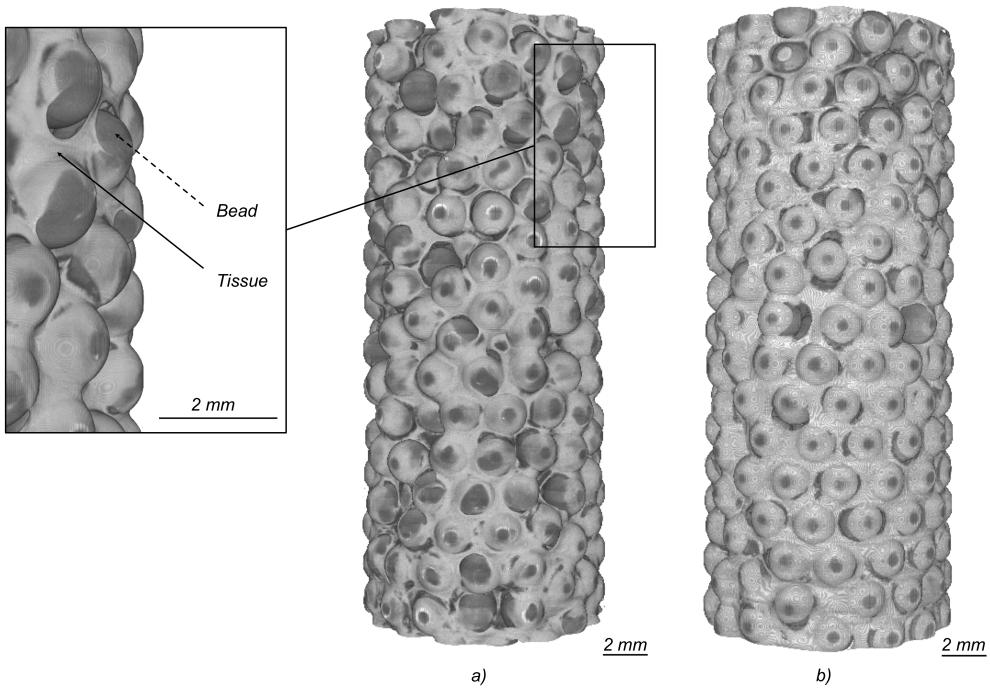

Figure 2: 3D views obtained by X-ray micro-tomography of the tissue on the scaffold after two weeks (a) and three weeks (b) of culture at a flow rate of 20 ml/min. The beads appear in dark grey (dashed arrow) and the tissue in light grey (black arrow). Scale bar, 2 mm.

The difference between the external and internal cell proliferation is shown in Fig. 3b which represents a slice of the bioreactor with a flow rate of 30 ml/min after three weeks. It can be seen that the tissue close to the bioreactor wall (colored in yellow) is denser than the tissue in the core (colored in blue). This phenomenon, observed in all the experiments, is also clearly illustrated in Fig. 3c where the intensity, that we define as the grey value of a pixel, of the cellular phase is summed over the entire stack. In order to support these observations, we quantify the averaged relative difference of intensity between the tissue in the core of the bioreactor and the envelope for all samples cultured three weeks. Two regions are identified: an annular region corresponding mainly to the tissue envelope previously described, and an inner

disk region representing the core of the bioreactor. Due to some heterogeneous arrangement of the beads in the vertical direction, the inner region is defined using two different radii R_1 and R_2. This corresponds to two regions (annular and disk) per radius. The thickness of the annular region amounts to about either one or two bead radii. We first determine the averaged relative difference of intensity between the tissue in the annular region and the tissue in the disk region considering the first radius R_1. The results provided in Table 1 are obtained for all samples cultured three weeks. The relative comparison of mean intensity between the core and the periphery are of the order of 50% in most cases. Of particular note, the average of 42.2% is mainly due to the heterogeneous arrangement of the beads in the vertical direction. Indeed, considering the second radius R_2, this relative difference amounts to 51.3%.

Additional scans of bioreactor inlets and outlets for experiments carried out with a flow rate of 30 ml/min show that the envelope actually encompasses the whole packing of beads (Fig. 4).

Flow rate	Sample	$R_1 = 10.13$ mm		
		Mean relative difference	Standard deviation	Average
20 ml/min	1	55.0%	5.3%	54.0%
	2	53.0%	4.4%	
30 ml/min	1	53.7%	9.2%	48.0%
	2	42.2%	10.3%	

Table 1: Averaged relative difference of intensity between the tissue in the annular region and the tissue in the disk region for a radius R_1 of 10.13 mm, for all samples cultured three weeks.

As shown below, this preferential tissue growth is related to the geometrical heterogeneities of the scaffold. These heterogeneities are due to the spatial distribution of the spherical beads at the vicinity of the wall (parietal region). This disordered arrangement in the parietal region is characterized by a local increase of the porosity and permeability values, both being therefore dependent on the radial coordinate. The consequence of these heterogeneities is an increase of

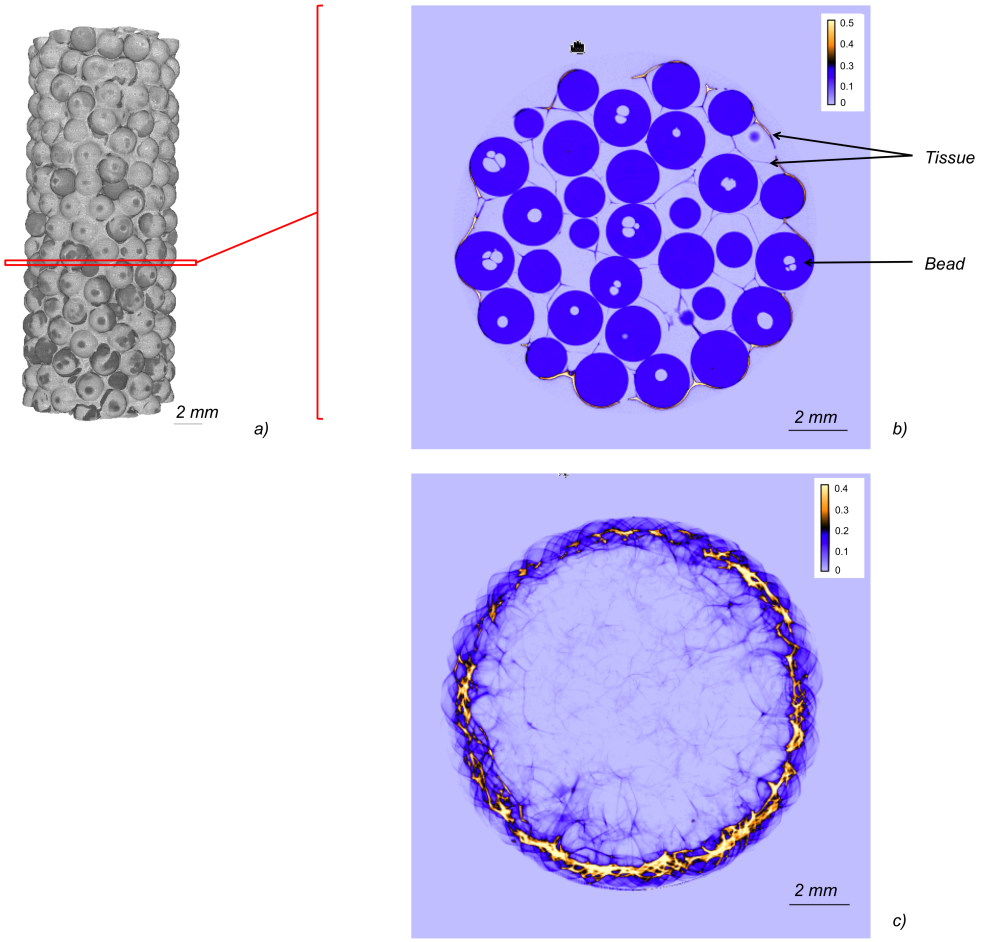

Figure 3: Visualization obtained by X-ray micro-tomography of the tissue on the scaffold after three weeks of culture at a flow rate 30 ml/min. (a) 3D side view. (b) 2D representative slide (intensity normalized with respect to the maximum intensity). (c) Sum over the whole stack of pixel intensity in the cellular region (relative to the maximum intensity).

the flow rate close to the wall leading to a more intense local flow. This *channeling effect* [50] gives rise to an increase of both nutrient transport and local shear stress, which results in a stronger mechanical stimulation of the cells in the parietal region and therefore in an increased proliferation. As a matter of fact, Cruel et al. [32] noticed radial heterogeneities of the fluid shear stress at the beads surface for bead granular packings. More specifically, we locate these heterogeneities at the bioreactor periphery. This mechanism can also be described at the bioreactor scale (macroscopic scale) where the averaged filtration velocity V in the direction of the flow (z-component) is governed by Darcy's law [51]:

$$0 = -\frac{dP}{dz} - \frac{\mu}{K}V \tag{1}$$

In Eq. (1), μ is the dynamic viscosity and K is the permeability coefficient in the direction

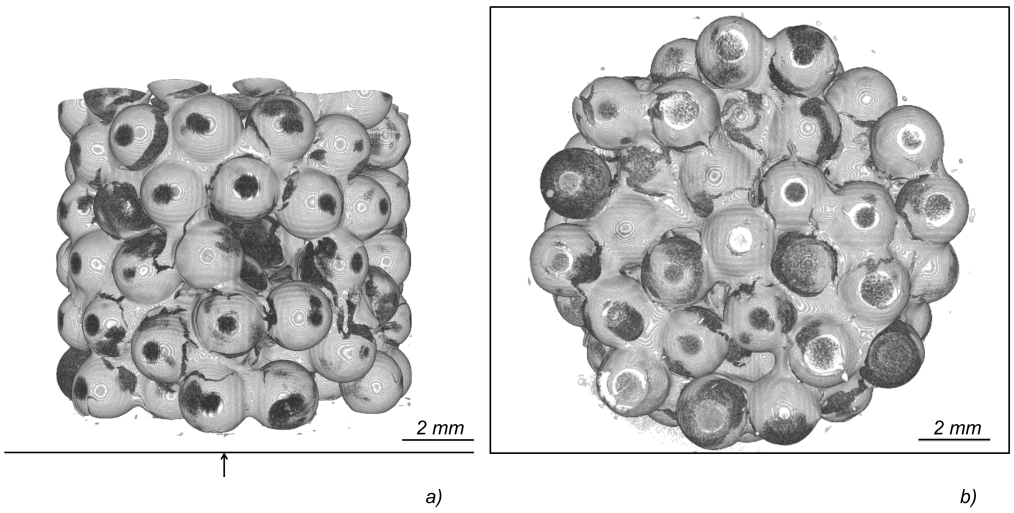

Figure 4: 3D views obtained by X-ray micro-tomography of the tissue on the scaffold at fluid inlet after three weeks of culture at a flow rate of 30 ml/min. (a) 3D side view. (b) 3D bottom view.

of the flow which depends on the radial coordinate r. For a porous media composed by mono dispersed spherical beads, the permeability is given by the Kozeny-Carman relationship $\overline{K} = \overline{\varepsilon}^3 d^2/180(1-\overline{\varepsilon})^2$ [52] where $\overline{\varepsilon}$ represents the average porosity and d the diameter of the beads. Therefore, Eq. (1) clearly shows that this *channeling effect* is explicitly dependent on the beads diameter. It is important to recall that Darcy's law is relevant if the local Reynolds number ($Re = \sqrt{\overline{K}}V/\nu$) is lower than 1. This is the case for our bioreactor where $\overline{\varepsilon} = 0.35$, $\overline{K} = 2 \cdot 10^{-9}\mathrm{m}^2$ and $Re = 0.16$. This estimation has been done for the maximum flow rate ($30\,\mathrm{ml.min}^{-1}$). Therefore, according to Eq. (1), for a given pressure gradient, the filtration velocity V continuously increases with the permeability K. It is worth mentioning that the thickness of the channeling region is of the order of $\sqrt{\overline{K}}$ and that the flow field non-uniformities in this region are negligible if the ratio d/D is very small compared to 1 (with d the beads diameter and D the bioreactor inner diameter) [50]. In our bioreactors, d/D is of the order of 0.1, which makes necessary to take into account the presence of a *channeling effect* in the analysis.

The above analysis leads to an important design principle for perfusion bioreactors using beads, or more generally granular scaffolds: the intensity of the channeling effect can be modulated according to specific bioreactor application by adjusting the ratio between the scaffold beads size and chamber diameter. For instance, if one aims to have homogeneous local flow rate across the scaffold, small beads and large chamber diameters should be used. On the contrary, if an application requires a large flow rate at the scaffold surrounding, bigger beads might be more appropriate.

3.2 Shear-stress pattern promotes crater-shaped tissue at early culture time

After one week of culture, the experiments show that whatever the flow rates, the tissue partly covers the beads with a crater-like shape. Indeed, we observe tissue overgrowths on the beads around circular areas devoid of cells and located in the narrowed fluid areas (Fig. 5). In order to investigate this formation of craters, we employ computational fluid dynamics to assess the local wall shear stress induced by the flow on the scaffold beads.

We numerically compute the shear stress field for a stationary laminar viscous flow through an idealized three-dimensional arrangement of nine identical spheres in a cylindrical channel. The radius of the channel is 2.7 mm while the radius of spheres is 1 mm. Flow properties are close to those of water at ambient temperature and the imposed inlet velocity is 0.001 m/s. Under these conditions, the associated Reynolds number is of the order 1 and therefore the fluid flow is laminar. Numerical simulations are performed using Comsol Multiphysics (version 4.3b). Figure 6 represents the isovalues of the shear stress field at the surface of the spheres. As expected, the maxima are located in the narrow fluid regions. Importantly, we find that the locations and form of the shear stress maxima obtained numerically correspond to the locations and the form of the crater-like tissue observed experimentally.

It is well known that the proliferation of mechanosensitive cells, including fibroblasts, is enhanced by the flow-induced shear stress. But this stimulation is clearly limited by the intensity of the stress. For high intensity values, cell detachment (which is also material-

dependent) [53] can be observed but cellular growth is probably prevented before reaching this limit. In the numerical simulations, the higher flow rate (30 ml/min) the maximum shear stress obtained is about 0.1 Pa which is close to the detrimental value (0.3 Pa) obtained by Truskey and Proulx [53] for fibroblasts NIH-3T3 seeded on glass. Note that this value is of the same order of magnitude as the detrimental shear stress obtained for osteoblasts by Leclerc et al. [54]. Although our numerical simulations ignore the presence of tissue on the beads, they provide useful insights into the determination of the spatial distribution of the tissue by the shear stress field in the perfusion bioreactor. Keeping the global flow rate constant through the growth chamber, the coupling of tissue growth with the laminar flow would lead to an intensification of the flow and an expected increase of the fluid shear stress.

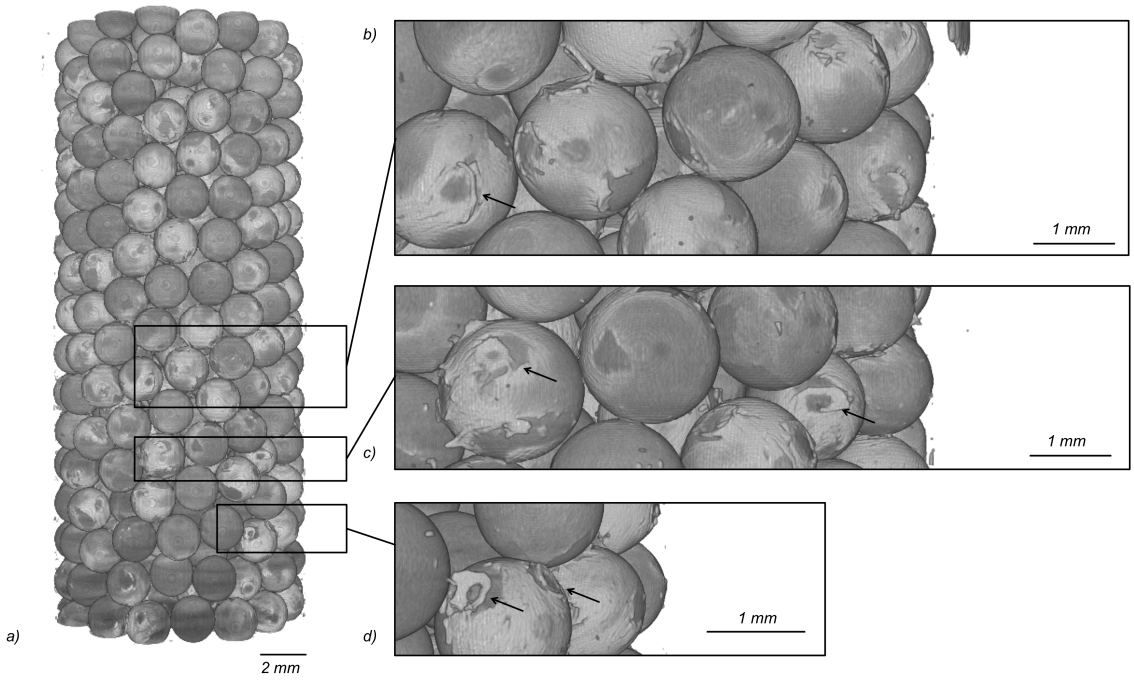

Figure 5: 3D views obtained by X-ray micro-tomography of the tissue on the scaffold after one week of culture at flow rate of 30 ml/min. (a) 3D side view. (b)(c)(d) Close-up views.

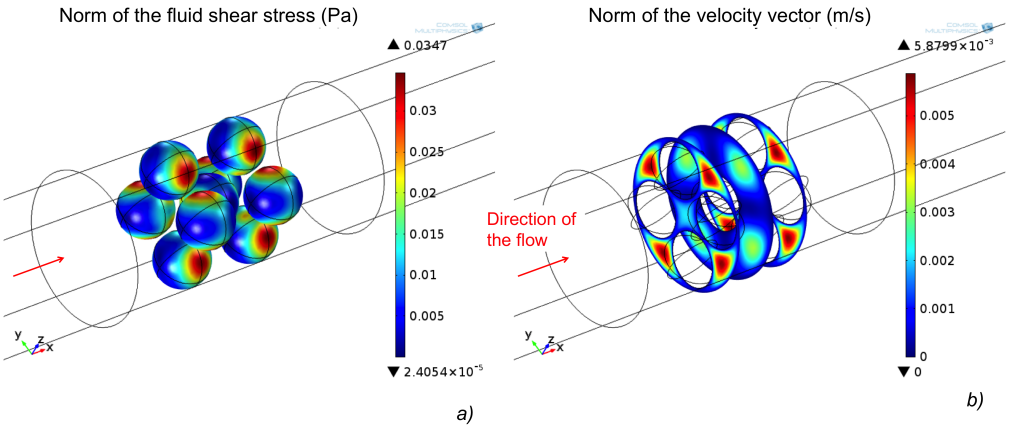

Figure 6: Numerical simulation of a laminar flow around a symmetrical arrangement of nine beads for an inlet velocity of 0.001 m.s^{-1}. (a) Norm of the fluid shear stress on the beads surface. (b) Norm of the fluid velocity vector.

3.3 Biomechanical interpretation of tissue morphology evolution

After one week of culture, the tissue has partly covered the beads with a crater-like shape (Fig. 5b,c,d). After two weeks, it clearly appears in Fig. 7b that the tissue grows by building "bridges" between the beads with concave and smooth interfaces. Such shapes are interpreted as the result of curvature minimization [29, 55, 56]. In other words, this results from the contribution of a tension line between the anchoring points and due to the acto-myosin cable along the edge of the tissue, balanced by a surface tension which comes from the global contractility of the cells [57].

Figure 7 also shows that the density of the tissue at the interface with the culture medium is higher than in the center of the "bridges". It seems that this phenomenon is related to the fact that cells in this interfacial region are mechanically stimulated by the shear stress induced by the flow of the medium. Interestingly, Kollmannsberger et al. [31] and Granet et al. [2] showed that cell proliferation preferentially occurs at the tissue-medium interface, where a higher

mechanical stimulation results in a higher cell proliferation rate [58]. The graph presented in Fig. 7e shows that this behavior is more pronounced in the parietal region presumably due to the *channeling effect* (Fig. 7d).

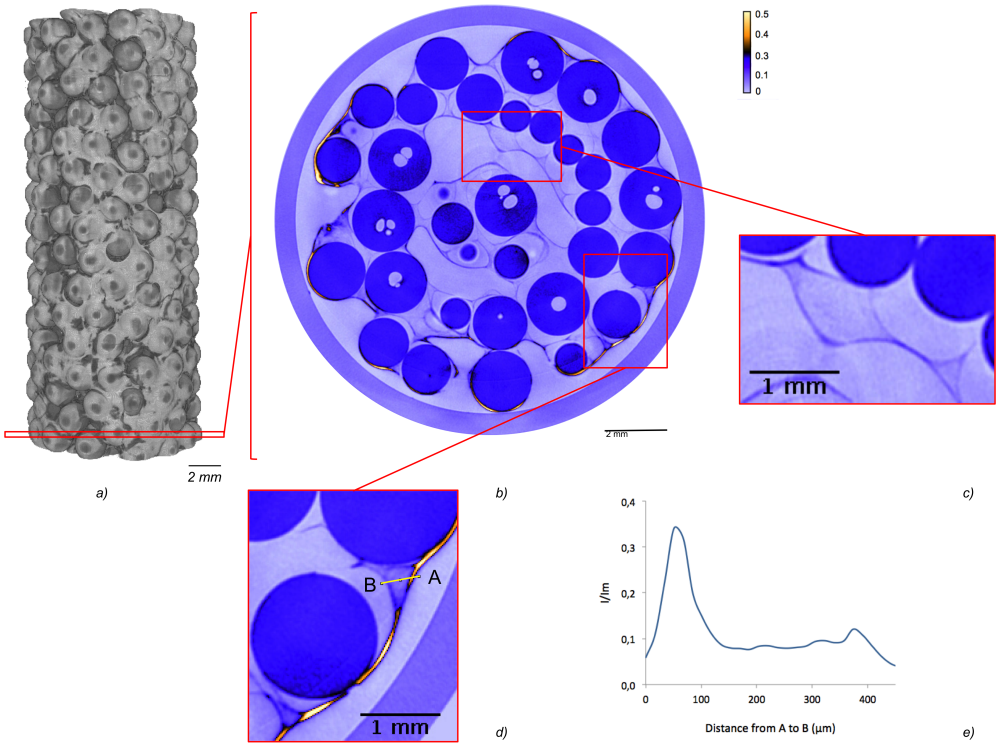

Figure 7: Visualization obtained by X-ray micro-tomography of the tissue on the scaffold after two weeks of culture at a flow rate 20 ml/min. (a) 3D side view. (b) 2D representative slide (intensity normalized with respect to the maximum intensity Im). (c)(d) Close-up views (e) Variation of the relative intensity I/I_m associated to each pixels along the yellow line drawn on (d).

Finally, it is worth recalling that cell contractility has also an important impact on the tissue morphology. Indeed, the evolution of the tissue depends on the balance between cell-cell and cell-scaffold interactions. After one week of culture, the formation of a few narrower "rings" where the tissue is partly ripped off (Fig. 5b,c,d) suggests that the tissue is subjected to considerable tensions. Such tears in the tissue have been observed with keratinocytes [59] and fibroblasts [60] forming suspended bridges and have been attributed to cell contractility. In addition, images of bioreactors cultured three weeks clearly show that the tissue has a dense sheet-like shape whatever the location in the bioreactors (Fig. 3), presumably as the result of tissue contraction. This phenomenon is also either initiated or complete after two weeks of culture all along the bioreactors (Fig. 7c). The detachment of the tissue from the scaffold

suggests that cell adhesion forces to the substrate are too weak to counterbalance the traction forces due to cell contractility.

4 Conclusion

In this work, we used a combination of tissue engineering, X-ray micro-tomography imaging, and fluid mechanics simulations to relate tissue morphology and local fluid flow conditions in a model perfusion bioreactor. The model bioreactor consisted of fibroblasts cells grown on a scaffold made of a stack of beads in a perfusion chamber.

Our results highlight the heterogeneous distribution of the cells as the consequence of a *channeling effect* in the bioreactor. Because of the particular arrangement of the bead packing and the subsequent higher porosity and permeability at the periphery of the bioreactor, the flow is more intense in the channel at the periphery. In our model bioreactor, this effect results in a preferred proliferation around the bead stack and the formation of a very dense envelope of tissue. The dimensions of the beads and bioreactor determine the importance of these boundary effects: a small bead to bioreactor diameter ratio means a weak *channeling effect*.

Furthermore, we identify crater-shaped tissue patterns at early culture times. We show that this morphology resembles the distribution of fluid shear stress on beads, highlighting the importance of local fluid flow on tissue development.

Finally, we find that after one, two and three weeks of culture, the tissue adopts very distinct morphologies, and attribute these observations to the simultaneous growth and contraction of the connective tissue as it grows.

By providing insights into the coupling between tissue development and fluid flow in a perfusion bioreactor, this work has potential implications in the effective design of bioreactors relying on hydrodynamic stimulii for tissue engineering.

Acknowledgments

This work has been financially supported by the French *Agence Nationale de la Recherche* through the *Investissements d'avenir* program (ANR-10-EQPX-37 MATMECA Grant) and the *Fondation pour la Recherche Médicale* (FRM FDT201805005480).

We thank Pascal Silberzan (Institut Curie) for kindly providing the NIH-3T3 cell line and Stéphane Roux (LMT, ENS Paris-Saclay) for his kind help regarding image post-processing.

Conflict of interest

The authors have no conflict of interest to declare and all co-authors confirm agreement with the final statement. All authors have been appropriately disclosed according to the policy of the Journal.

Ethical statement

There are no animal experiments carried out for this article.

References

[1] Gordana Vunjak-Novakovic, Lisa E Freed, Robert J Biron, and Robert Langer. Effects of mixing on the composition and morphology of tissue-engineered cartilage. *AIChE Journal*, 42(3):850–860, 1996. doi: 10.1002/aic.690420323.

[2] C Granet, N Laroche, L Vico, C Alexandre, and MH Lafage-Proust. Rotating-wall vessels, promising bioreactors for osteoblastic cell culture: comparison with other 3d conditions. *Medical and Biological Engineering and Computing*, 36(4):513–519, 1998. doi: 10.1007/BF02523224.

[3] Bertrand David, Dominique Bonnefont-Rousselot, Karim Oudina, Marie-Christelle Degat, Mickael Deschepper, Véronique Viateau, Morad Bensidhoum, Christian Oddou, and Hervé Petite. A perfusion bioreactor for engineering bone constructs: an in vitro and in vivo study. *Tissue Engineering Part C: Methods*, 17(5):505–516, 2011. doi: 10.1089/ten.tec.2010.0468.

[4] Andrew B Yeatts and John P Fisher. Tubular perfusion system for the long-term dynamic culture of human mesenchymal stem cells. *Tissue Engineering Part C: Methods*, 17(3):337–348, 2010. doi: 10.1089/ten.tec.2010.0172.

[5] Gregory N Bancroft, Vassilios I Sikavitsas, Juliette Van Den Dolder, Tiffany L Sheffield, Catherine G Ambrose, John A Jansen, and Antonios G Mikos. Fluid flow increases mineralized matrix deposition in 3d perfusion culture of marrow stromal osteoblasts in a dose-dependent manner. *Proceedings of the National Academy of Sciences*, 99(20):12600–12605, 2002. doi: 10.1073/pnas.202296599.

[6] Andrew B Yeatts and John P Fisher. Bone tissue engineering bioreactors: dynamic culture and the influence of shear stress. *Bone*, 48(2):171–181, 2011. doi: 10.1016/j.bone.2010.09.138.

[7] Warren L Grayson, Mirjam Fröhlich, Keith Yeager, Sarindr Bhumiratana, M Ete Chan, Christopher Cannizzaro, Leo Q Wan, X Sherry Liu, X Edward Guo, and Gordana Vunjak-

Novakovic. Engineering anatomically shaped human bone grafts. *Proceedings of the National Academy of Sciences*, 107(8):3299–3304, 2010. doi: 10.1073/pnas.0905439106.

[8] Warren L Grayson, Darja Marolt, Sarindr Bhumiratana, Mirjam Fröhlich, X Edward Guo, and Gordana Vunjak-Novakovic. Optimizing the medium perfusion rate in bone tissue engineering bioreactors. *Biotechnology and bioengineering*, 108(5):1159–1170, 2011. doi: 10.1002/bit.23024.

[9] Delphine Antoni, Hélène Burckel, Elodie Josset, and Georges Noel. Three-dimensional cell culture: a breakthrough in vivo. *International journal of molecular sciences*, 16(3): 5517–5527, 2015. doi: 10.3390/ijms16035517.

[10] Matthew James Robeson et al. Model of a tubular perfusion bioreactor using computational fluid dynamics. 2015.

[11] P Sanaei, LJ Cummings, SL Waters, and IM Griffiths. Curvature-and fluid-stress-driven tissue growth in a tissue-engineering scaffold pore. *Biomechanics and modeling in mechanobiology*, pages 1–17, 2018.

[12] Julie Glowacki, Shuichi Mizuno, and Joel S Greenberger. Perfusion enhances functions of bone marrow stromal cells in three-dimensional culture. *Cell Transplantation*, 7(3): 319–326, 1998. doi: 10.1016/S0963-6897(98)00003-7.

[13] S Scaglione, D Wendt, S Miggino, A Papadimitropoulos, M Fato, R Quarto, and I Martin. Effects of fluid flow and calcium phosphate coating on human bone marrow stromal cells cultured in a defined 2d model system. *Journal of Biomedical Materials Research Part A*, 86(2):411–419, 2008. doi: 10.1002/jbm.a.31607.

[14] T Scheper, R Faurie, and J Thommel. Advances in biochemical engineering/biotechnology. *Advances in Biochemical Engineering Biotechnology*, 109, 2008. doi: 10.1007/978-3-642-28478-6.

[15] Ivan Martin, David Wendt, and Michael Heberer. The role of bioreactors in tissue engineering. *TRENDS in Biotechnology*, 22(2):80–86, 2004. doi: 10.1016/j.tibtech.2003.12.001.

[16] A Wayne Orr, Brian P Helmke, Brett R Blackman, and Martin A Schwartz. Mechanisms of mechanotransduction. *Developmental cell*, 10(1):11–20, 2006. doi: 10.1016/j.devcel.2005.12.006.

[17] Benoit Ladoux and Alice Nicolas. Physically based principles of cell adhesion mechanosensitivity in tissues. *Reports on Progress in Physics*, 75(11):116601, 2012. doi: 10.1088/0034-4885/75/11/116601.

[18] Kathleen M Reich, Carol V Gay, and John A Frangos. Fluid shear stress as a mediator of osteoblast cyclic adenosine monophosphate production. *Journal of cellular physiology*, 143(1):100–104, 1990. doi: 10.1002/jcp.1041430113.

[19] Akira Katsumi, A Wayne Orr, Eleni Tzima, and Martin Alexander Schwartz. Integrins in mechanotransduction. *Journal of Biological Chemistry*, 279(13):12001–12004, 2004. doi: 10.1074/jbc.R300038200.

[20] Zhenhai Li, Hyunjung Lee, and Cheng Zhu. Molecular mechanisms of mechanotransduction in integrin-mediated cell-matrix adhesion. *Experimental cell research*, 349(1):85–94, 2016. doi: 10.1016/j.yexcr.2016.10.001.

[21] Elizabeth S Haswell, Rob Phillips, and Douglas C Rees. Mechanosensitive channels: what can they do and how do they do it? *Structure*, 19(10):1356–1369, 2011. doi: 10.1016/j.str.2011.09.005.

[22] Ryan J McCoy and Fergal J O'Brien. Influence of shear stress in perfusion bioreactor cultures for the development of three-dimensional bone tissue constructs: a review. *Tissue Engineering Part B: Reviews*, 16(6):587–601, 2010. doi: 10.1089/ten.teb.2010.0370.

[23] Michaela Brosig. *Mechanotransduction in fibroblasts*. PhD thesis, University_of_Basel, 2011.

[24] Nicolas F Berbari, Amber K O'Connor, Courtney J Haycraft, and Bradley K Yoder. The primary cilium as a complex signaling center. *Current Biology*, 19(13):R526–R535, 2009. doi: 10.1016/j.cub.2009.05.025.

[25] SA Korossis, F Bolland, JN Kearney, J Fisher, E Ingham, et al. Bioreactors in tissue engineering. *Topics Tissue Eng*, 2(8):1–23, 2005.

[26] Benoit Ladoux and René-Marc Mège. Mechanobiology of collective cell behaviours. *Nature Reviews Molecular Cell Biology*, 18(12):743, 2017. doi: 10.1038/nrm.2017.98.

[27] Cécile M Bidan, Philip Kollmannsberger, Vanessa Gering, Sebastian Ehrig, Pascal Joly, Ansgar Petersen, Viola Vogel, Peter Fratzl, and John WC Dunlop. Gradual conversion of cellular stress patterns into pre-stressed matrix architecture during in vitro tissue growth. *Journal of The Royal Society Interface*, 13(118):20160136, 2016. doi: 10.1098/rsif.2016.0136.

[28] Mahmut Selman Sakar, Jeroen Eyckmans, Roel Pieters, Daniel Eberli, Bradley J Nelson, and Christopher S Chen. Cellular forces and matrix assembly coordinate fibrous tissue repair. *Nature communications*, 7:11036, 2016. doi: 10.1038/ncomms11036.

[29] Monika Rumpler, Alexander Woesz, John WC Dunlop, Joost T van Dongen, and Peter Fratzl. The effect of geometry on three-dimensional tissue growth. *Journal of the Royal Society Interface*, 5(27):1173–1180, 2008. doi: 10.1098/rsif.2008.0064.

[30] Puja Sharma, Colin Ng, Aniket Jana, Abinash Padhi, Paige Szymanski, Jerry SH Lee, Bahareh Behkam, and Amrinder S Nain. Aligned fibers direct collective cell migration to engineer closing and nonclosing wound gaps. *Molecular Biology of the Cell*, 28(19):2579–2588, 2017. doi: 10.1091/mbc.e17-05-0305.

[31] Philip Kollmannsberger, Cécile M Bidan, John WC Dunlop, Peter Fratzl, and Viola Vogel. Tensile forces drive a reversible fibroblast-to-myofibroblast transition during tissue growth in engineered clefts. *Science advances*, 4(1):eaao4881, 2018. doi: 10.1126/sciadv.aao4881.

[32] Magali Cruel, Morad Bensidhoum, Cécile Nouguier-Lehon, Olivier Dessombz, Pierre Becquart, Hervé Petite, and Thierry Hoc. Numerical study of granular scaffold efficiency to convert fluid flow into mechanical stimulation in bone tissue engineering. *Tissue Engineering Part C: Methods*, 21(9):863–871, 2015. doi: 10.1089/ten.tec.2014.0648.

[33] Md Shakhawath Hossain, DJ Bergstrom, and XB Chen. Prediction of cell growth rate over

scaffold strands inside a perfusion bioreactor. *Biomechanics and modeling in mechanobiology*, 14(2):333–344, 2015.

[34] Ayelet Lesman, Yaron Blinder, and Shulamit Levenberg. Modeling of flow-induced shear stress applied on 3d cellular scaffolds: Implications for vascular tissue engineering. *Biotechnology and bioengineering*, 105(3):645–654, 2010.

[35] Michele M Nava, Manuela T Raimondi, and Riccardo Pietrabissa. A multiphysics 3d model of tissue growth under interstitial perfusion in a tissue-engineering bioreactor. *Biomechanics and modeling in mechanobiology*, 12(6):1169–1179, 2013.

[36] Cécile M Bidan, Krishna P Kommareddy, Monika Rumpler, Philip Kollmannsberger, Yves JM Bréchet, Peter Fratzl, and John WC Dunlop. How linear tension converts to curvature: geometric control of bone tissue growth. *PloS one*, 7(5):e36336, 2012.

[37] Yann Guyot, Ioannis Papantoniou, FP Luyten, and Liesbet Geris. Coupling curvature-dependent and shear stress-stimulated neotissue growth in dynamic bioreactor cultures: a 3d computational model of a complete scaffold. *Biomechanics and modeling in mechanobiology*, 15(1):169–180, 2016.

[38] M Chabanon, H Duval, O Francais, Bruno Lepioufle, E Perrin, Benoit Goyeau, and B David. Discrete model combined with mimetic microfluidic chips to study cell growth in porous scaffold under flow conditions. *Computer methods in biomechanics and biomedical engineering*, 15(sup1):25–26, 2012. doi: 10.1080/10255842.2012.713699.

[39] Morgan Chabanon, Hervé Duval, Jérôme Grenier, Claire Beauchesne, Benoît Goyeau, and Bertrand David. Histological method to study the effect of shear stress on cell proliferation and tissue morphology in a bioreactor. *Tissue Engineering and Regenerative Medicine*, 2019. doi: 10.1007/s13770-019-00181-3.

[40] Roman Thibeaux, Herve Duval, Benjamin Smaniotto, Elsa Vennat, David Néron, and Bertrand David. Assessment of the interplay between scaffold geometry, induced shear stresses, and cell proliferation within a packed bed perfusion bioreactor. *Biotechnology progress*, 2019.

[41] J Harris. Fibroblasts and their transformations: the connective-tissue cell family. *Molecular Biology of the Cell*, pages 1179–1193, 1994.

[42] James H-C Wang, Bhavani P Thampatty, Jeen-Shang Lin, and Hee-Jeong Im. Mechanoregulation of gene expression in fibroblasts. *Gene*, 391(1):1–15, 2007. doi: 10.1016/j.gene.2007.01.014.

[43] B. David, H. Petite, and V. Myrtil. Reacteur pour la mise en oeuvre d'un procede de culture de tissus osseux, January 22 2009. URL `https://encrypted.google.com/patents/WO2009010661A2?cl=fr`. WO Patent App. PCT/FR2008/000,846.

[44] Andrew B Yeatts, Carly N Gordon, and John P Fisher. Formation of an aggregated alginate construct in a tubular perfusion system. *Tissue Engineering Part C: Methods*, 17 (12):1171–1178, 2011.

[45] David E Orr and Karen JL Burg. Design of a modular bioreactor to incorporate both perfusion flow and hydrostatic compression for tissue engineering applications. *Annals of Biomedical Engineering*, 36(7):1228, 2008.

[46] Nilay J Lakhkar, Jeong-Hui Park, Nicola J Mordan, Vehid Salih, Ivan B Wall, Hae-Won Kim, Scott P King, John V Hanna, Richard A Martin, Owen Addison, et al. Titanium phosphate glass microspheres for bone tissue engineering. *Acta biomaterialia*, 8(11):4181–4190, 2012.

[47] Nihal Engin Vrana, Agnès Dupret-Bories, Philippe Schultz, Christian Debry, Dominique Vautier, and Philippe Lavalle. Titanium microbead-based porous implants: bead size controls cell response and host integration. *Advanced healthcare materials*, 3(1):79–87, 2014.

[48] R Thibeaux, E Perrin, B Smaniotto, H Duval, E Vennat, D Neron, and B David. Using x-ray computed tomography for quantification of cell proliferation within a perfusion bioreactor. *Computer methods in biomechanics and biomedical engineering*, 18(sup1):2072–2073, 2015. doi: 10.1080/10255842.2015.1069568.

[49] Caroline A Schneider, Wayne S Rasband, and Kevin W Eliceiri. Nih image to imagej: 25 years of image analysis. *Nature methods*, 9(7):671, 2012. doi: 10.1038/nmeth.2089.

[50] Massoud Kaviany. *Principles of heat transfer in porous media*. Springer Science & Business Media, 2012. doi: 10.1007/978-1-4684-0412-8.

[51] Henry Darcy. *Les fontaines publiques de la ville de Dijon: exposition et application...* Victor Dalmont, 1856.

[52] Philip Crosbie Carman. Fluid flow through granular beds. *Trans. Inst. Chem. Eng.*, 15: 150–166, 1937.

[53] George A Truskey and Timothy L Proulx. Relationship between 3t3 cell spreading and the strength of adhesion on glass and silane surfaces. *Biomaterials*, 14(4):243–254, 1993. doi: 10.1016/0142-9612(93)90114-H.

[54] Eric Leclerc, B David, L Griscom, Bruno Lepioufle, T Fujii, Pierre Layrolle, and C Legallaisa. Study of osteoblastic cells in a microfluidic environment. *Biomaterials*, 27(4):586–595, 2006. doi: 10.1016/j.biomaterials.2005.06.002.

[55] Cécile M Bidan, Krishna P Kommareddy, Monika Rumpler, Philip Kollmannsberger, Peter Fratzl, and John WC Dunlop. Geometry as a factor for tissue growth: towards shape optimization of tissue engineering scaffolds. *Advanced healthcare materials*, 2(1):186–194, 2013. doi: 10.1002/adhm.201200159.

[56] P Kollmannsberger, CM Bidan, JWC Dunlop, and P Fratzl. The physics of tissue patterning and extracellular matrix organisation: how cells join forces. *Soft matter*, 7(20): 9549–9560, 2011. doi: 10.1039/C1SM05588G.

[57] Ilka B Bischofs, Franziska Klein, Dirk Lehnert, Martin Bastmeyer, and Ulrich S Schwarz. Filamentous network mechanics and active contractility determine cell and tissue shape. *Biophysical journal*, 95(7):3488–3496, 2008. doi: 10.1529/biophysj.108.134296.

[58] Celeste M Nelson, Ronald P Jean, John L Tan, Wendy F Liu, Nathan J Sniadecki, Alexander A Spector, and Christopher S Chen. Emergent patterns of growth controlled by multicellular form and mechanics. *Proceedings of the National Academy of Sciences of the United States of America*, 102(33):11594–11599, 2005. doi: 10.1073/pnas.0502575102.

[59] Sri Ram Krishna Vedula, Hiroaki Hirata, Mui Hoon Nai, Yusuke Toyama, Xavier Trepat, Chwee Teck Lim, Benoit Ladoux, et al. Epithelial bridges maintain tissue integrity during collective cell migration. *Nature materials*, 13(1):87, 2014. doi: 10.1038/nmat3814.

[60] Olivier M Rossier, Nils Gauthier, Nicolas Biais, Wynn Vonnegut, Marc-Antoine Fardin, Philip Avigan, Evan R Heller, Anurag Mathur, Saba Ghassemi, Michael S Koeckert, et al. Force generated by actomyosin contraction builds bridges between adhesive contacts. *The EMBO journal*, 29(6):1055–1068, 2010. doi: 10.1038/emboj.2010.2.